PERGAMON

International Journal of Heat and Mass Transfer 43 (2000) 209–218

International Journal of HEAT and MASS TRANSFER

www.elsevier.com/locate/ijhmt

Liquid cooling for a multichip module using Fluorinert liquid and paraffin slurry

Mingoo Choi, Keumnam Cho*

School of Mechanical Engineering, Sungkyunkwan University, 300 Chunchun-dong, Changan-ku, Suwon 440-746, South Korea

Received 2 February 1999; received in revised form 10 April 1999

Abstract

The objective of the present study was to investigate the effect of phase change material on heat transfer enhancement in a multichip module application. The parameters studied in the present study include the mass fraction of paraffin slurry, the heat flux of simulated VLSI chips and channel Reynolds numbers. The size of paraffin slurry particles was within 10–40 μm. The local heat transfer coefficients for the paraffin slurry were larger than those for water. The paraffin slurry showed an effective cooling performance at high heat fluxes. The paraffin slurry with a mass fraction of 5% showed the most efficient cooling performance when the heat transfer and the pressure drop in the test section were considered simultaneously. The present experimental data at the fourth and sixth rows gave an excellent agreement with the values predicted by the Malina and Sparrow's correlation, and a new empirical correlation for the water and paraffin slurry with a mass fraction of 5% was proposed at the first and sixth rows for a channel Reynolds number over 3000. © 1999 Elsevier Science Ltd. All rights reserved.

Keywords: Multichip module; Paraffin slurry; Heat transfer coefficient

1. Introduction

Packaging has always played an important role in determining the overall speed, cost and reliability of high-speed communication systems such as supercomputers, mainframes, and military electronics. Moreover, increasing circuit count and density in circuits have been adding further demands on packaging. In order to minimize the delay, chips must be placed close together. Thus, the multichip module (MCM) technology has been introduced to significantly improve performance by minimizing the level of packaging. An MCM is a packaging technique that places several semiconductor chips, interconnected in a high density substrate, into a single package. MCMs offer several advantages such as reduced weight, reduced size, increased reliability and enhanced performance. As the density of an active silicon increases, so does the density of heat generation. Not only producing the individual chips from 50 to 100 W cm^{-2} is problematic, but the problem of thermal management is further compounded by the multichip modules even at a heat flux of 25 W cm^{-2} [1–5]. Thus, the thermal management is a key issue on the overall designs of MCM assemblies. Several strategies have been developed for controlling and removing the heat generated in MCMs. These include advanced air and liquid cooling schemes. The heat removal rate in the air-cooling scheme is limited by the convection coefficient. A liquid cooling method using a liquid fluorocarbon solution has been used for the cooling of multichip mod-

* Corresponding author. Tel.: +82-331-290-7445; fax: +82-331-290-5849.

E-mail address: keumnam@yurim.skku.ac.kr (K. Cho)

0017-9310/00/$ - see front matter © 1999 Elsevier Science Ltd. All rights reserved.
PII: S0017-9310(99)00137-4

Nomenclature

A	surface area [m^2]
C_p	specific heat at constant pressure [kJ kg^{-1} K^{-1}]
D_h	hydraulic diameter [m]
EF	enhancement factor, Eq. (9)
f	Fanning friction factor, $(\Delta P D_h)/(2\rho L U^2)$
h	heat transfer coefficient [W m^{-2} K^{-1}]
k	thermal conductivity [W m^{-1} K^{-1}]
L	length [m]
Nu	Nusselt number, $(hD_h)/k_f$
ΔP	pressure drop [Pa]
Pr	Prandtl number, $(\mu_f C_p)/k_f$
q''	heat flux, $V^2/(RA_s)$ [W cm^{-2}]
R	resistance [ohms]
Re	Reynolds number, $(\rho_f U D_h)/\mu_f$
T	temperature [°C]
U	average velocity [m s^{-1}]
V	voltage [V]
x	mass fraction of paraffin slurry [%]

Greek symbols

μ	viscosity [N s m^{-2}]
ρ	density [kg m^{-3}]

Subscripts

f	working fluid
m	mixture of paraffin slurry and water
p	paraffin
s	chip
sat	saturation
sub	subcooling
w	water

Superscript

+	dimensionless

ules. Fluorocarbon is electrically insulating and chemically stable. The liquid cooling method can be classified as the forced convection cooling method [6,7], pool boiling cooling method [8,9], forced convection boiling cooling method [10,11]. However, the direct liquid cooling method is recently replaced by the indirect liquid cooling method due to both the maintenance problem of the system and the thermal shock produced by thermal hysteresis. This requires the effective indirect liquid cooling method that can keep the surface temperature of the MCMs with a high heat flux within a certain temperature limit. Therefore, the present study deals with the application of a phase change material (PCM) slurry as an alternative indirect liquid cooling method. Some experimental studies showed that the convective heat transfer coefficient as well as the thermal capacity of a working fluid increased by using PCM slurry [12,13]. The potential benefits of using PCMs in the thermal control of electronic systems are as follows: (a) increased heat capacity of the heat transfer fluid due to the latent heat of a fusible material in suspension, and (b) increased heat transfer coefficients at fluid and solid surface due to particle rotations in turbulent flow and the role of latent heat of particles. Numerical and experimental studies have been performed on the application of PCMs for the passive thermal control of electronic systems [14–16]. These studies reported that the natural convection of molten PCMs inside a cavity or cylinder enhances the overall heat transfer. In these studies, organic PCMs were used for the active cooling of the MCMs, especially *n*-paraffins, because paraffins are stable and nontoxic chemicals. They are compatible with packaging materials, noncorrosive, and inert.

The objective of the present study was to investigate (1) the effect of PCM on heat transfer enhancement in the MCM application and (2) the effects of various experimental parameters on the cooling performance of the MCM with a high heat flux. The experimental results are compared with existing correlations under a continuous heating condition, and new correlations under a discrete heating condition are provided.

2. Experimental apparatus and procedure

Present experiments were performed with three different types of solutions: water, PF-5060 (a dielectric liquid manufactured by 3 M Co.) and a paraffin slurry. PF-5060 is an alternative coolant for FC-72, and its typical properties are shown and compared with FC-72 and water in Table 1. Note that the viscosity of PF-5060 is much smaller than that of water.

A commercial grade paraffin ($C_{22}H_{46}$) was used, which has a melting temperature of 43.6°C and a fusion energy of 175.6 kJ kg^{-1} measured by a DSC (Differential Scanning Calorimeter). The measurement uncertainty of melting temperature by the DSC was 0.8°C from the calibration data with distilled water. Thermophysical properties of the paraffin are presented in Table 2. In order to make fine paraffin particles, an emulsifier was used. Paraffin is an organic PCM and consists of a mixture of normal alkane. Paraffin slurry was made by cooling inside a bath,

Table 1
Thermophysical properties of the Fluorinert liquids and water (at 25°C and 1 atm)

Property	PF-5060	FC-72	Water
Boiling point, °C	56	56	100
Density (liquid), g cm^{-3}	1.68	1.68	1.0
Viscosity, cs	0.4	0.4	0.9
Surface tension, dyne cm^{-1}	12	12	72
Vapor pressure, kPa	30	30	3.3
Heat of vaporization, kJ kg^{-1}	88.2	88.2	2268
Specific heat, kJ kg^{-1} °C^{-1}	1.05	1.05	4.2
Thermal conductivity, W m^{-1} K^{-1}	0.057	0.057	0.610

where distilled water, liquid paraffin and emulsifier were mixed. Water and paraffin are immiscible each other. The molecules of emulsifier are composed of a hydrophilic head group and hydrophobic tail. If a very small amount of the emulsifier is injected to the mixture of water and paraffin, the paraffin becomes a dispersed phase, and water becomes a continuous phase.

A schematic diagram of the present experimental apparatus is shown in Fig. 1. The apparatus consisted of a main test section, a power supply, a plate-type heat exchanger, a constant temperature bath, a pump, a mass flow meter, a data acquisition system. The test section consisted of a rectangular channel and a multichip module as shown in Fig. 2. The rectangular channel with an aspect ratio of 0.2 shows the most efficient cooling performance for a fully developed laminar single phase flow in case of a heated top wall with uniform heat flux. Since the present study deals with a fully developed turbulent flow and discrete heating at the top wall, results reported in the literature [17] can-

Table 2
Thermophysical properties of paraffin

Property	Value
Melting temperature, °C	43.6
Heat of fusion, kJ kg^{-1}	176.8
Specific heat, kJ kg^{-1} °C^{-1}	
Liquid (60°C)	2.52
Solid	2.98
Thermal conductivity, W m^{-1} K^{-1}	
Liquid (60°C)	0.17
Solid	0.24
Density, g cm^{-3}	
Liquid (60°C)	0.76
Solid	0.82
Viscosity (60°C), cP	3.14
Molecular weight, g mol^{-1}	332

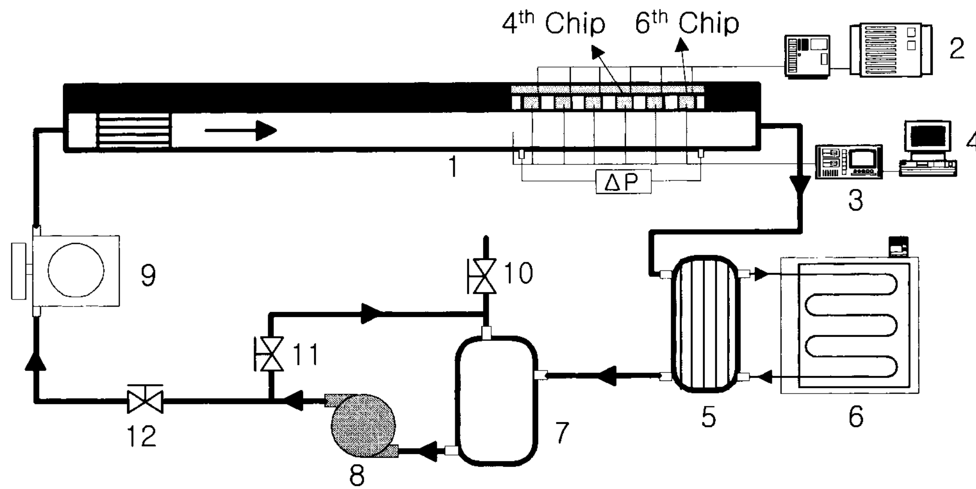

1. Rectangular channel
2. DC power supply
3. Data acquisition system
4. Personal computer
5. Plate-type heat exchanger
6. Constant temp. bath
7. Receiver tank
8. Pump
9. Mass flow meter
10 ~ 12. Valves

Fig. 1. Schematic diagram of the present experimental apparatus.

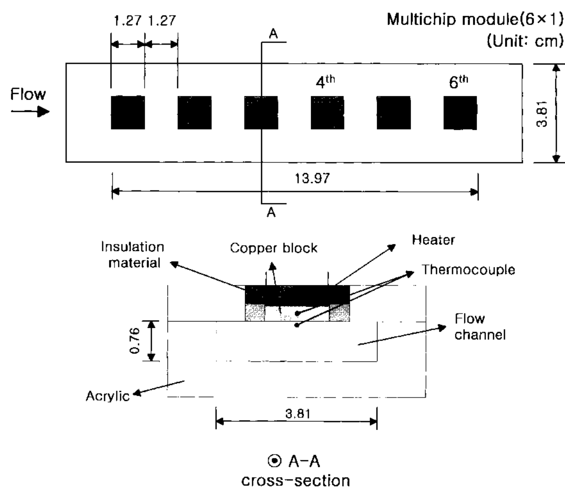

Fig. 2. Details of the present test section.

not directly be applied to the present study. Since no data on the relation between aspect ratio and cooling performance were reported for the fully developed turbulent flow, the aspect ratio of 0.2 (7.6 ± 0.05 mm $\times$ 38.1 ± 0.05 mm) was chosen. The hydraulic diameter of the present rectangular channel was 1.26 cm.

The multichip module had an in-line 6×1 array of discrete heat sources simulating VLSI chips, and it was flush-mounted on the top wall of a horizontal acrylic rectangular channel. The multichip module was located at a downstream location 50 times of the hydraulic diameter from the inlet of the test section, where flow was hydrodynamically fully developed. A honeycomb section was located at the inlet of the channel to make flow uniform. Two static pressure taps were located at the bottom wall just before and after the MCM and connected to an U-tube manometer to measure pressure drop across the MCM. A heating wire with a resistance of $18.6 \pm 0.2\Omega$ m^{-1} was attached to each copper block and electrically isolated from the copper block by thermal silicon for heat source. Six heating wires on the chips were connected in parallel to a power supply with an accuracy of ± 0.03 V to supply a uniform heat flux to each heater. Each heat source had a square shape with a size of 1.27 cm, a typical size of a VLSI chip. The distance between two adjacent chips was 1.27 cm. A copper heat sink with a thickness of 6 mm was attached at the bottom of each chip, and the top side was thermally insulated by fiberglass to force the heat flow only to the channel. The copper heat sink was a square shape of the same size as the heater. The maximum temperature difference at three positions on a copper heat sink was approximately 0.5°C. The temperature of the copper heat sink and the fluid temperature just below (0.5 mm) the copper heat sink surface were measured by type T thermocouples inserted through machined holes. The thermocouples were calibrated within an accuracy of ± 0.15°C by a standard RTD.

A conduction analysis was performed on both the heat source and the substrate using the values of thermal conductivities for copper block (386 W m^{-1} K^{-1}), acrylic (0.2 W m^{-1} K^{-1}), thermal silicon (1.6 W m^{-1} K^{-1}), and insulation material (0.02 W m^{-1} K^{-1}). The heat loss from the heater to the surroundings ranged from 2.1 to 3.3% in the whole experimental range and was compensated in the calculation of heat flux on heater.

Three key experimental parameters were the heat flux, channel Reynolds number, and mass fraction of paraffin slurry. The heat flux varied from 10 to 40 W cm^{-2}, the channel Reynolds number ranged from 3000 to 20,000, and the mass fraction of paraffin slurry varied from 0 (water) to 10%. The heat flux was obtained by dividing the heat supplied to each chip by the chip area. The Reynolds number was calculated by using the hydraulic diameter of the rectangular channel with an aspect ratio of 0.2. The inlet temperature of the test section was set to 15°C for all runs.

Local heat transfer coefficients were calculated by dividing the heat flux supplied to each chip by the temperature difference between the surface temperature of the chip and the fluid temperature measured at a location 0.5 mm below the chip as shown in the following equation:

$$h = \frac{q''}{(T_s - T_f)}. \tag{1}$$

The determination of a bulk temperature in the rectangular channel requires temperature and velocity profiles in 2-dimensional directions. This made it difficult to determine the bulk temperature. Thus, the convective heat transfer coefficients were obtained by using fluid temperature just below a heat sink instead of the bulk temperature. The heat flux was obtained by using the supplied voltage and the resistance of the heater.

The error analysis showed that the error range of the heat flux was ± 1.93%, whereas that in the local heat transfer coefficient estimation was ± 3.8%.

3. Method to determine particle size and properties of paraffin slurry

The size of a paraffin slurry was controlled by the amount of an emulsifier. The density of paraffin is smaller than that of water, so that the particles float. Therefore, the size of the paraffin particles had to be small enough to prevent from clogging flow loop.

When the concentration of the emulsifier to the mass fraction of the paraffin was 3.3%, the size of the paraffin slurry particles ranged from 10 to 40 μm. The photographs of the paraffin slurry with a mass fraction of 10% are shown in Fig. 3.

The density and specific heat of the paraffin slurry are obtained by the following equations [18]:

$$\frac{1}{\rho_m} = \frac{\frac{x}{100}}{\rho_p} + \frac{1-\frac{x}{100}}{\rho_w} \quad (2)$$

$$\frac{1}{C_{p,m}} = \frac{\frac{x}{100}}{C_{p,p}} + \frac{1-\frac{x}{100}}{C_{p,w}} \quad (3)$$

which can be used for the slurries of very fine, monosize, spherical particles. Lee and Shin [19] proposed a thermal conductivity correlation for a paraffin slurry

(a) Before experiment

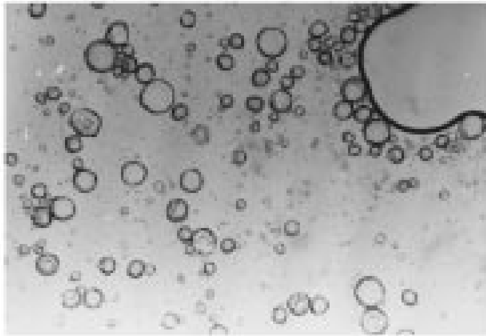

(b) After experiment

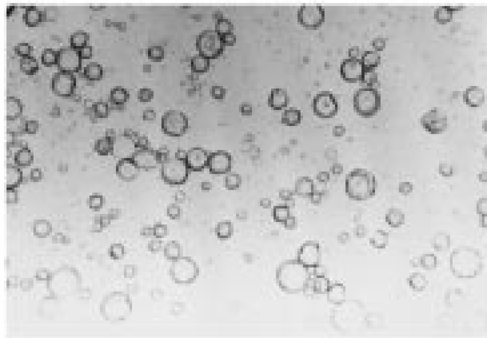

40μm

Fig. 3. Photographs of paraffin slurry with a mass fraction of 10%.

with the error range within ±3%, which is given as

$$\frac{k_m}{k_w} = \frac{2k_w + k_p - 0.023\left(\frac{\rho_m}{\rho_p}x\right)(k_w - k_p)}{2k_w + k_p + 0.023\left(\frac{\rho_m}{\rho_p}x\right)(k_w - k_p)}. \quad (4)$$

The relationship between the viscosity and concentration of the suspension of paraffin slurry with the error range within ±5% is proposed by the following equation [18]:

$$\frac{\mu_m}{\mu_w} = 1 + 2.5\frac{\rho_m}{\rho_p}\frac{x}{100} + 10.05\left(\frac{\rho_m}{\rho_p}\frac{x}{100}\right)^2 + 0.00273 \exp\left(16.6\frac{\rho_m}{\rho_p}\frac{x}{100}\right). \quad (5)$$

The viscosity of a paraffin-water emulsion above the melting temperature of a paraffin was obtained by the following equation [20] which is generally used for an emulsion:

$$\ln \mu_m = \frac{x}{100} \ln \mu_p + \left(1 - \frac{x}{100}\right) \ln \mu_w. \quad (6)$$

4. Results and discussion

Fig. 4 shows the apparent Fanning friction factor in the test section as a function of Reynolds number. The modified Blasius equation introduced by Jones [21] for rectangular ducts is described as

$$f = 0.079(Re^*_{D_h})^{-0.25} \quad (7)$$

where the Kozicki Reynolds number, $Re^*_{D_h}$, is defined

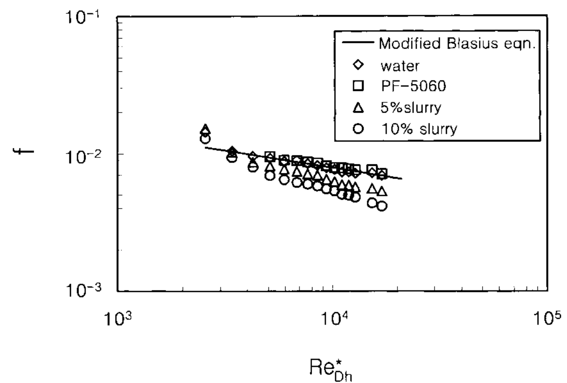

Fig. 4. Friction factor for water, PF-5060, 5% and 10% paraffin slurries in the present test section.

as

$$Re^*_{D_h} = a(\rho U D_h/\mu). \quad (8)$$

Note that the value of a in Eq. (8) is constant, whose value depends on the aspect ratio of a rectangular channel. For example, it was 0.85 for an aspect ratio of 0.2.

Measured friction factors for water and PF-5060 at two different heat fluxes of 10 and 30 W cm^{-2} gave good agreement with the values predicted by the modified Blasius equation within $\pm$6%. The pressure drop data for water were approximately 4 times larger than those for PF-5060, but apparent Fanning friction factors for water and PF-5060 showed little difference as shown in Fig. 4. The reason is that the pressure drop is proportional to the apparent Fanning friction factor and the square of average velocity. The average velocity for water is about two times larger than that for PF-5060 at the same Reynolds number since the kinematic viscosity of water is 2.25 times larger than that for PF-5060 as shown in Table 1. Pressure drop data for the paraffin slurry were larger than those for water, whereas apparent Fanning friction factors for the paraffin slurry were smaller than those for water. The reason is that the average velocity for the paraffin slurry increases as the mass fraction of the paraffin slurry increases at the same Reynolds number since the kinematic viscosity of the paraffin slurry is greater than that of water.

Fig. 5 shows the heat flux ranges that can be removed from the chips with respect to the chip surface temperatures at the first and sixth rows of the multichip module at a channel Reynolds number of 20,000. For PF-5060 and water, the temperature difference between the first and sixth rows increased as heat flux increased. The chip surface temperatures for water were lower than those for PF-5060 since the specific heat and thermal conductivity for PF-5060 were approximately 25% and 10.6% of those for water. The chip surface temperatures for water were lower by 20.9–21.5°C than those for PF-5060 at a heat flux of 10 W cm^{-2}. As the heat flux increased to 30 W cm^{-2}, the boiling at the chip surface became more vigorous than the case with a heat flux of 10 W cm^{-2} and thus, the chip surface temperatures for water were lower by 14.2–16.2°C than those for PF-5060. When heat flux was over 40 W cm^{-2}, the heater surface temperature for PF-5060 abruptly increased over 300°C, and the experiment became meaningless. The chip surface temperatures decreased as the mass fraction increased at the first and sixth rows, and the surface temperature decreased more rapidly at a high heat flux than at a low heat flux. The chip surface temperatures for the paraffin slurry with a mass fraction of 5% were lower than those for water by 4.6–6.1°C for a heat flux of 10 W cm^{-2}, and by 11.2–11.4°C for a heat flux of 40 W cm^{-2}. The chip surface temperatures reduced slowly as the mass fraction increased over the whole heat flux range, and was notable at the sixth row. This means that the melting quantity of paraffin particles near the chip surface did not increase linearly although the mass fraction of paraffin increased.

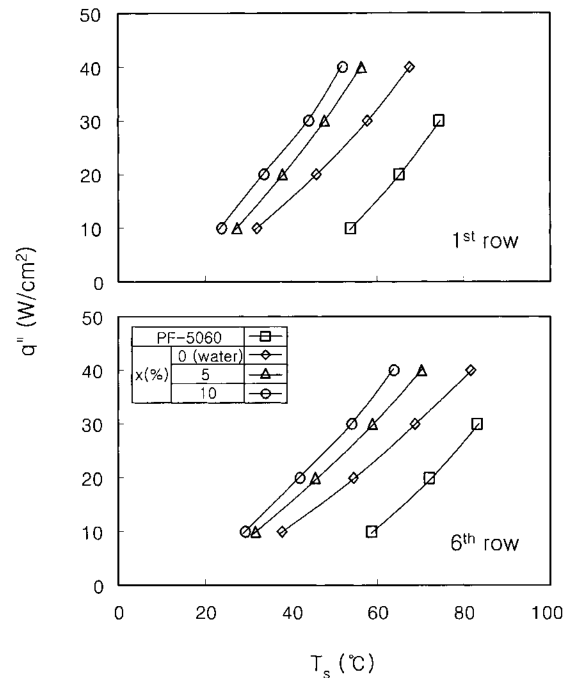

Fig. 5. Removable heat flux with respect to chip surface temperatures (Re_{D_h} = 20,000).

Fig. 6 shows boiling curves for PF-5060 at the first and sixth rows for an average velocity of 0.386 m s^{-1} (Re_{D_h} = 11,200) at the inlet of the test section and for the case of a subcooling of 41°C. Note that the subcooling (ΔT_{sub}) is a temperature difference between the saturation temperature of PF-5060 (T_{sat} = 56°C) and inlet temperature (T_i = 15°C). At low heat fluxes below approximately 5 W cm^{-2}, a single phase convection was a dominant heat transfer mode even though the surface temperature was over the saturation temperature. The single phase convection effect at the first heater was larger than that at the sixth heater since upstream heaters continuously affected the sixth heater. The temperature overshoot was 3.5°C and 2.6°C at the first and sixth heaters, respectively. The temperature overshoot is defined as the difference between the onset temperature of nucleate boiling (ONB) and the temperature obtained from the boiling curve at the same heat flux with ONB.

Local heat transfer coefficients were obtained by using the chip surface temperature and fluid tempera-

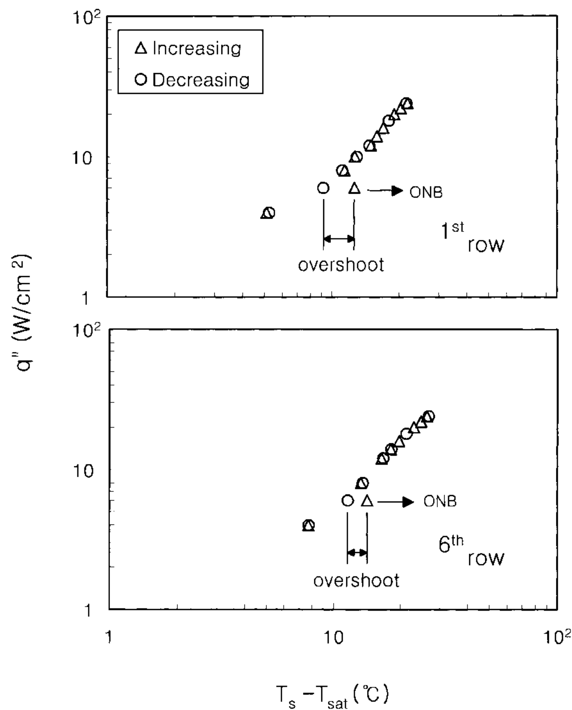

Fig. 6. Boiling curve for PF-5060 ($Re_{D_h}=11{,}200$ ($U_i=0.38$ ms^{-1}), $\Delta T_{sub}=41°C$).

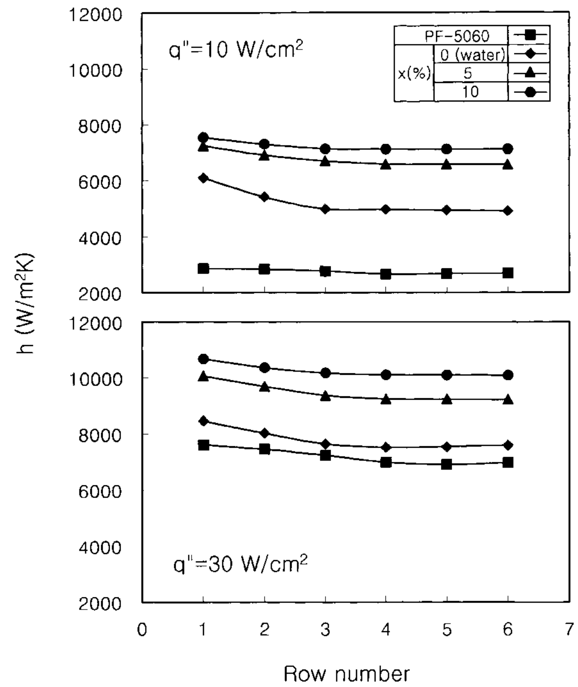

Fig. 7. Local heat transfer coefficient with respect to row number ($Re_{D_h}=20{,}000$).

ture 0.5 mm below the chip surface. Fig. 7 shows the local heat transfer coefficients with respect to the row number for a channel Reynolds number of 20,000 and heat fluxes of 10 and 30 W cm^{-2}. The local heat transfer coefficients reached an uniform value approximately after the fourth row (located at a distance seven times of the chip length) regardless of coolants. This means that the thermally fully developed condition was reached after the fourth row. Garimella and Eibeck [22] also observed the attainment of fully developed conditions after the fourth row. The local heat transfer coefficients for water at a heat flux of 10 W cm^{-2} were about 1.7–2.1 times larger than those for PF-5060. As the heat flux increased to 30 W cm^{-2}, the local heat transfer coefficients for water were larger by 5.5–11.2% than those for PF-5060. The reason is that as the heat flux increased up to a certain value, a subcooled nucleate boiling near a heater surface made the local heat transfer coefficient for PF-5060 to increase. The local heat transfer coefficients for the paraffin slurry with a mass fraction of 5% were larger by 18.7–34.1% at the first row and by 22.7–42.6% at the sixth row than those for water. The reason for the heat transfer enhancements was due to both the particle migration and subsequent collision against wall in turbulent flow and the latent heat of PCM. Heat transfer phenomena for turbulent slurry flow are complex and need to be better understood. Transverse migration of particles adjacent to a surface can aid in both disrupting the laminar sublayer and increasing the heat transfer coefficient. The latent heat of the PCM, which can be viewed as a form of specific heat, increases the heat transfer coefficient because the heat transfer coefficient increases as the one-third power of the specific heat for turbulent flow.

Fig. 8 shows the dimensionless local heat transfer coefficients (h^+) at the first and sixth rows with respect to the mass fraction of the paraffin slurry for the case of a Reynolds number of 20,000. The dimensionless local heat transfer coefficient is defined as the ratio of the local heat transfer coefficient for the paraffin slurry to that for water. As the mass fraction increased from 0 to 10%, the dimensionless local heat transfer coefficients at heat fluxes of 10 and 40 W cm^{-2} slowly increased when the mass fraction increased over 5%. In particular, for a heat flux of 40 W cm^{-2} the dimensionless local heat transfer coefficients increased slowly at the sixth row such as 25, 18, 7, 3% as the mass fraction of the paraffin slurry increased. This indicates that the local heat transfer coefficients reached an asymptotic value beyond a mass fraction of 10% when the Reynolds number was 20,000 and the heat flux varied from 10 to 40 W cm^{-2}. The variation of the local heat transfer coefficients at heat fluxes of 10 and 40 W cm^{-2} was more remarkable at the sixth row than that

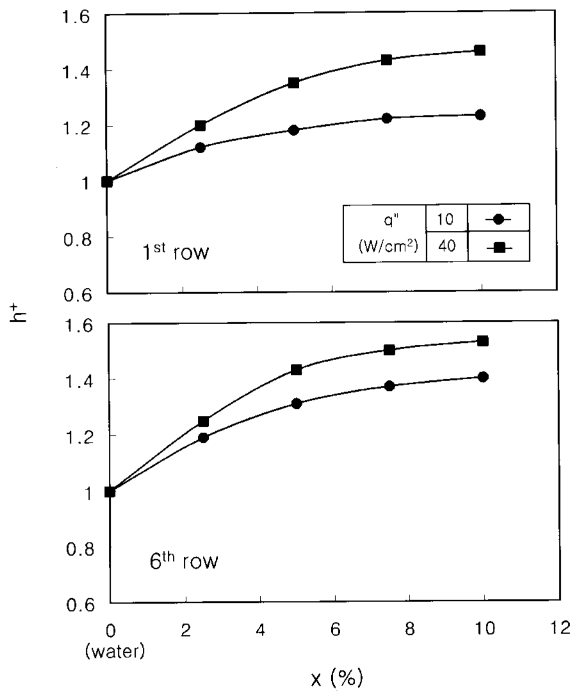

Fig. 8. Dimensionless local heat transfer coefficient at the first and sixth rows (Re_{D_h} = 20,000).

at the first row, as the mass fraction of the paraffin slurry increased. This means that the effect of the latent heat of the paraffin slurry on the local heat transfer coefficient was larger at the downstream than that at the upstream. At the sixth row, the cooling effect by the sensible heat of the paraffin slurry decreased since the temperature of the working fluid increased. However, since the fluid temperature reached the melting temperature of the paraffin, the cooling effect by the latent heat increased downstream.

Fig. 9 shows enhancement factors (EFs) obtained by using the local heat transfer coefficient and the pressure drop at a Reynolds number of 20,000. Note that the *EF* is defined as

$$EF = \frac{h^+}{\Delta P^+} \tag{9}$$

where ΔP^+ is the ratio of the pressure drop for the paraffin slurry to that for water. For heat fluxes of 10 and 40 W cm^{-2}, the EFs for the paraffin slurry with a mass fraction of 5% showed the largest value. This means that the paraffin slurry with a mass fraction of 5% shows the most efficient cooling performance when the heat transfer and pressure drop in the test section were considered simultaneously.

The local Nusselt number was obtained by using local heat transfer coefficients. The local Nusselt number data for water were compared with well-known correlations [23–26] for both the hydrodynamically and thermally fully developed turbulent forced convection in circular ducts for liquids with variable properties.

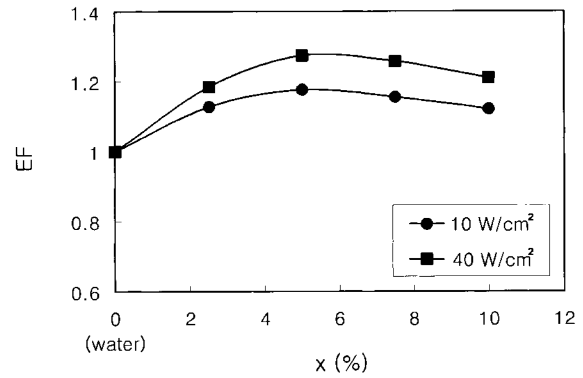

Fig. 9. Enhancement factor at the 6th row (Re_{D_h} = 20,000).

Fig. 10 shows the test results in the form of *Nu* vs *Re* at the fourth and sixth rows for heat fluxes of 10 and 30 W cm^{-2}. Even though the slopes of the experimental results are slightly lower than those from Malina and Sparrow's correlation, the values predicted by the Malina and Sparrow's correlation among the other correlations gave the best agreement with the present experimental data. For a heat flux of 10 W

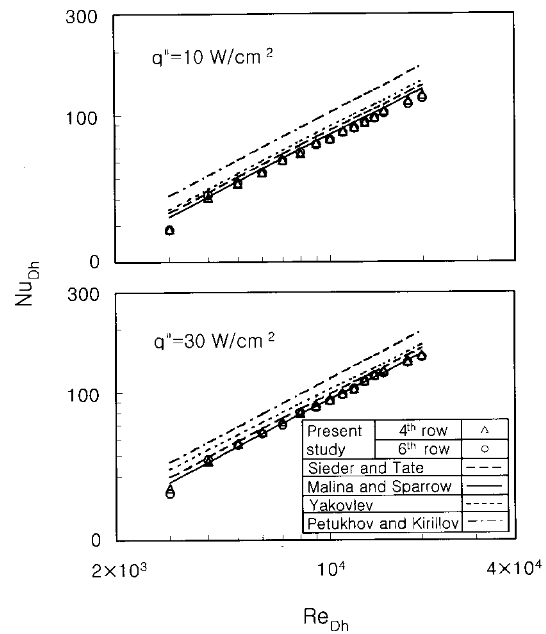

Fig. 10. Comparison of Nusselt number data with the values predicted by various correlations for water.

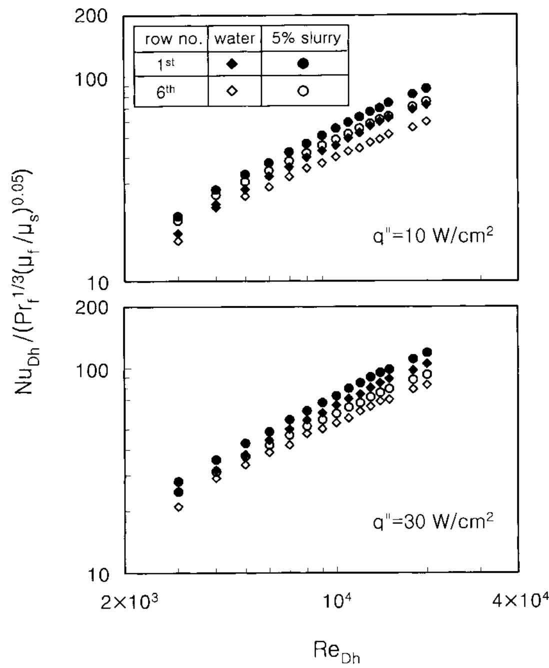

Fig. 11. Nusselt number with respect to Reynolds number for water and 5% paraffin slurry.

cm^{-2}, the local Nusselt number was lower by 2.2–7.6% than the values predicted by the Malina and Sparrow's correlation, and for a heat flux of 30 W cm^{-2}, the Malina and Sparrow's correlation agreed with the present experimental data with a maximum deviation of $\pm$3%.

Fig. 11 shows the Nusselt numbers at the first and sixth rows with respect to the channel Reynolds number by using a viscosity ratio exponent of 0.05, and a Prandtl number exponent of 1/3. The local Nusselt numbers at the first row were larger than those at the sixth row since the first row was in the thermally developing condition. The Nusselt numbers for the paraffin slurry with a mass fraction of 5% were larger by 9.7–27.8% than those for water at a heat flux of 30 W cm^{-2}.

Table 3
Values of coefficient in Eq. (10)

Heat flux, W cm^{-2}	Mass fraction, %	Row no.	C	m
10	0	1	0.083	0.692
		6	0.089	0.662
	5	1	0.057	0.746
		6	0.047	0.747
30	0	1	0.099	0.694
		6	0.086	0.698
	5	1	0.062	0.766
		6	0.059	0.760
Malina and Sparrow			0.023	0.8

An empirical correlation was obtained at the first and sixth rows for water and the paraffin slurry with a mass fraction of 5% which showed the most effective cooling performance. The new correlation based on the present results is provided by the following form:

$$\frac{Nu_{Ls}}{Pr_{\mathrm{f}}^{1/3}(\mu_{\mathrm{f}}/\mu_{\mathrm{s}})^{0.05}} = CRe_{D_{\mathrm{h}}}^{\mathrm{m}} \tag{10}$$

where the values of C and m are presented in Table 3 and the channel Reynolds number is over 3000.

5. Conclusions

A summary of the present study is given below.

1. The size of paraffin slurry particles could be maintained in a range of 10–40 μm by using an emulsifier.
2. Friction factors for both water and PF-5060 gave good agreement with the values predicted by the modified Blasius equation within $\pm$6%, and the apparent Fanning friction factors for the paraffin slurry were smaller than those for either water or PF-5060.
3. Chip surface temperatures for water were lower than those for PF-5060. Chip surface temperature differences between water and PF-5060 were 14.2–16.2°C at a heat flux of 30 W cm^{-2}. The chip surface temperatures for the paraffin slurry with a mass fraction of 5% were lower by 4.6–11.4°C than those for water.
4. Local heat transfer coefficients for the paraffin slurry were larger than those for water due to the disruption of laminar sublayer by paraffin particles, the direct heat transfer due to particle–wall impact, and the role of the latent heat of the paraffin.
5. Thermally fully developed conditions were observed after the fourth row (located at a distance seven times of the chip length), and the paraffin slurry showed an effective cooling performance downstream of an MCM and at a high heat flux of 40 W cm^{-2}.
6. Paraffin slurry with a mass fraction of 5% showed the most efficient cooling performance when both heat transfer and pressure drop in the test section were considered simultaneously.
7. The present experimental data after the fourth row gave the best agreement with the values predicted by the Malina and Sparrow's correlation among several correlations, and a new empirical correlation for water and the paraffin slurry with a mass frac-

tion of 5% was provided at the first and sixth rows for channel Reynolds numbers over 3000.

Acknowledgements

The authors wish to acknowledge the financial support of the Korea Research Foundation (1997-001-E-00011). This work was supported in part by the Korea Science and Engineering Foundation through the RRC for Advanced Climate Control Technology at Sun Moon University.

References

[1] A. Bar-Cohen, Recent advances in passive immersion cooling of high power devices, in: E. Suhir, M. Shiratori, Y.C. Lee (Eds.), Proceedings of the Pacific Rim/ASME International and Intersociety Electronic and Photonic Packaging Conference, Hawaii, ASME, 1997, pp. 2053–2054.

[2] W. Nakayama, Liquid-cooling of electronic equipment: where does it offer viable solutions?, in: E. Suhir, M. Shiratori, Y.C. Lee (Eds.), Proceedings of the Pacific Rim/ASME International and Intersociety Electronic and Photonic Packaging Conference, Hawaii, ASME, 1997, pp. 2045–2052.

[3] R.R. Tummala, Electronic packaging in the 1990's—a perspective from America, IEEE Comp. Hybrids Manuf. Technol. 14 (2) (1991) 262–271.

[4] T. Ohsaki, Electronic packaging in the 1990's—a perspective from Asia, IEEE Comp. Hybrids Manuf. Technol. 14 (2) (1991) 254–261.

[5] J.K. Hagge, State-of-the-art multichip modules for avionics, IEEE Comp. Hybrids Manuf. Technol. 15 (1) (1992) 29–41.

[6] E. Baker, Liquid cooling of microelectronic devices by free and forced convection, Microelectronics and Reliability 11 (1972) 213–222.

[7] F.P. Incropera, J.S. Kerby, D.F. Moffatt, S. Ramadhyani, Convection heat transfer from discrete heat sources in a rectangular channel, Int. J. Heat Mass Transfer 29 (1986) 1051–1058.

[8] I. Mudawar, T.M. Anderson, Parametric investigation into the effects of pressure, subcooling, surface augmentation and choice of coolant on pool boiling in the design of cooling systems for high power density electronic chips, ASME J. Electronic Packaging 112 (1990) 357–382.

[9] K.A. Park, A.E. Bergles, Natural convection heat transfer characteristics of simulated microelectronic chips, ASME J. Heat Transfer 109 (1987) 90–96.

[10] T.J. Heindel, S. Ramadhyani, F.P. Incropera, Liquid immersion cooling of a longitudinal array of discrete heat sources in protruding substrates: II—forced convection boiling, ASME J. Electronic Packaging 114 (1992) 63–70.

[11] I. Mudawar, D.E. Maddox, Enhancement of critical heat flux from high power microelectronic heat sources in a flow channel, ASME J. Electronic Packaging 112 (1990) 241–248.

[12] Y.I. Cho, E. Choi, H.G. Lorsch, A novel concept for heat transfer fluids used in district cooling systems, ASHRAE Trans. 97 (1991) 653–658.

[13] E. Choi, Y.I. Cho, H.G. Lorsch, Forced convection heat transfer with phase-change-material slurries: turbulent flow in a circular tube, Int. J. Heat Mass Transfer 37 (1994) 207–215.

[14] R. Chebi, P.A. Rice, J.A. Schwarz, Heat dissipation in microelectronic systems using phase change materials with natural convection, Chem. Eng. Commun. 69 (1988) 1–12.

[15] K.W. Snyder, An investigation of using a phase-change material to improve the heat transfer in a small electronic module for an airborne radar application, in: Proceedings of the International Electronic Packaging Conference, San Diego, 1991, pp. 276–303.

[16] D. Pal, Y.K. Joshi, Application of phase change materials to thermal control of electronic modules: a computational study, ASME J. Electronic Packaging 119 (1997) 40–50.

[17] J.P. Hartnett, M. Kostic, Heat transfer to Newtonian and non-Newtonian fluids in rectangular ducts, in: J.P. Hartnett, T.F. Irvine Jr (Eds.), Advances in Heat Transfer, Academic Press, New York, 1989, pp. 247–356.

[18] C.A. Shook, Slurry pipeline flow, in: P.A. Shamlou (Ed.), Processing of Solid-Liquid Suspensions, Butterworth-Heinemann, Oxford, 1993, pp. 287–309.

[19] S.H. Lee, S. Shin, Measurement of the shear rate-dependent thermal conductivity for suspension with microparticles, KSME(B) Trans. 22 (8) (1998) 1141–1151.

[20] R.C. Reid, J.M. Prausnitz, T.K. Sherwood, The Properties of Gases and Liquids, 3rd ed., McGraw-Hill, New York, 1977.

[21] O.C. Jones Jr, An improvement in the calculation of turbulent friction in rectangular ducts, ASME J. Fluid Engineering 98 (1976) 173–181.

[22] S.V. Garimella, P.A. Eibeck, Heat transfer characteristics of an array of protruding elements in single phase forced convection, Int. J. Heat Mass Transfer 33 (12) (1990) 2659–2669.

[23] E.N. Sieder, G.E. Tate, Heat transfer and pressure drop of liquids in tubes, Ind. Eng. Chem. 28 (1936) 1429–1453.

[24] J.A. Malina, E.M. Sparrow, Variable property, constant property and entrance region heat transfer results for turbulent flow of water and oil in a circular tube, Chem. Eng. Sci. 19 (1964) 953–962.

[25] D.G. Rogers, Forced convection heat transfer in single phase flow of a newtonian fluid in a circular pipe. CSIR Report CENG 322, Pretoria, South Africa, 1980.

[26] B.S. Petukhov, Heat transfer and friction in turbulent pipe flow with variable physical properties, in: J.P. Hartnett, T.F. Irvine Jr (Eds.), Advances in Heat Transfer, Academic Press, New York, 1970, pp. 505–564.